Functional analysis of SNP mutations leading to single amino acid substitution in NBCe1

Na^{+}-HCO_3^{-}共輸送体（NBCe1）の単一アミノ酸置換を伴うSNP変異体の機能解析

山崎　修

INDEX

Abstract

The electrogenic Na^+-HCO_3^- cotransporter NBCe1 encoded by *SLC4A4* plays essential roles in the regulation of intracellular/extracellular pH. Homozygous mutations in NBCe1 cause proximal renal tubular acidosis associated with ocular abnormalities. In the present study I tried to perform functional characterization of the 4 nonsynonymous single nucleotide polymorphisms (SNPs), E122G, S356Y, K558R, and N640I in NBCe1A. Functional analysis in *Xenopus* oocytes revealed that while the K558R variant had a significantly reduced transport activity corresponding to 47% of the wild-type activity, the remaining variants E122G, S356Y and N640I did not change the NBCe1A activity. Apparent Na^+ affinity of K558R was not different from that of wild-type NBCe1A. Immunohistological analyses in HEK293 cells and MDCK cells indicated that none of these SNPs changed the trafficking behaviors of NBCe1A. Functional analysis in HEK293 cells also revealed that only the K558R variant had a reduced transport activity, corresponding to 41 - 47% of the wild-type activity. From these results I conclude that among 4 SNPs only the K558R variant, which is predicted to lie in transmembrane segment 5, significantly reduces the NBCe1A activity without changing the trafficking behavior or the apparent extracellular Na^+ affinity.

Key Words: pRTA, SLC4A4, SNP, renal proximal tubules

Introduction

The regulation of extracellular and intracellular pH within the optimal ranges is essential for a variety of cellular functions. This task is accomplished by several acid/base transporters. Among them, the electrogenic Na^+-HCO_3^- cotransporter NBCe1 encoded by *SLC4A4* has three splice variants that mediate different physiological roles [1-3].

In 1997 Romero et al. [4] succeeded in molecular cloning of the renal Na^+-HCO_3^- cotransporter NBCe1. When expressed in *Xenopus* Oocytes, NBCe1 shows the very similar properties that have been characterized by previous physiological studies. Subsequently, it became apparent that NBCe1 has several variants: NBCe1A from kidney, NBCe1B from pancreas, and NBCe1C from brain. While the patterns of tissue distribution are different among these isoform, NBCe1A differs from NBCe1B only at the N-terminal region. In addition, NBCe1B is identical to NBCe1C at the amino acid level and differs only in its 5'-untranslated region. The human SLC4A4 gene is located on chromosome 4q21 [5].

The kidney-type cotransporter NBCe1A, predominantly expressed in the basolateral membrane of renal proximal tubules, mediates a majority of bicarbonate exit from renal proximal tubules, thereby performing an essential role in the systemic acid/base balance [1, 4, 6]. As shown in Fig. 1a, the first step of HCO_3^- absorption in renal proximal tubules is driven by the secretion of H^+ ions into the tubular lumen via Na^+/H^+ exchangers and/or via a H^+ ATPase pump which work in parallel. The secreted H^+ ions react with the filtered HCO_3^- to generate CO_2, which diffuses into the cells and recombines with the OH^- ions that were left behind during H^+ secretion, thus generating HCO_3^-. Both reactions, the disintegration of HCO_3^- in the tubular lumen and the

regeneration of HCO_3^- in the tubular cell, are catalyzed by carbonic anhydrase (CA), which is bound to the blush border membrane and is also dissolved in the cytoplasm. As the second step of HCO_3^- adsorption, a Na^+-HCO_3^- cotransporter has been identified in the peritubular cell membrane of both amphibian and mammalian renal proximal tubules [7-9]. Depending on its stoichiometry this cotransporter should be capable of exporting both HCO_3^- and Na^+ against their concentration differences from the cell into the peritubular fluid with the electrical cell membrane potential providing the driving force. From the effect of various divalent anions such as sulphite on Na^+-HCO_3^- cotransport, Soleimani and Aronson have postulated that the cotransporter actually transports 1 Na^+ plus 1 CO_3^{2-} plus 1 HCO_3^- per transport cycle [10]. This stoichiometry has been also confirmed in isolated proximal tubules [11].

On the other hand, the pancreas-type cotransporter NBCe1B, in which the first 41 amino acids of NBCe1A are replaced by the unique 85 amino acids, is widely expressed in different types of tissues including pancreatic ducts [12-16], intestinal tracts [17, 18], corneal endothelium and lens epithelium [19, 20], and astrocytes [21, 22]. Bicarbonate uptake into cells through NBCe1B is thought to be essential for the biological processes such as the maintenance of homeostasis in cornea and lens [19, 20], the pancreatic bicarbonate secretion [13, 15], and the regulation of local pH in the brain [21, 23].

The classical view of HCO_3^- secretion by the pancreatic duct cells had emphasized the roles of a basolateral Na^+ /H^+ exchanger, intracellular HCO_3^- formation catalyzed by carbonic anhydorase, and apical Cl^- / HCO_3^- exchangers [24]. However, a functional study in guinea pig pancreatic duct cells has shown that the Na^+-HCO_3^- cotransporter, which functions at $1Na^+$ to $2HCO_3^-$ stoichiometry, contributes ~75% of uptake during stimulation by secretin [25]. Recent studies indicate that HCO_3^- is taken up across the

basolateral membranes of the pancreatic duct via NBCe1 and is secreted across the apical membrane via cystic fibrosis transmembrane conductance regulator (CFTR) working in tandem with apical Cl^-/HCO_3^- exchangers [12, 13, 26, 27] as shown in Fig. 1b. In addition, Shumaker et al. [2] have shown that NBCe1B is responsible for secretin-stimulated HCO_3^- uptake into human pancreatic duct cells. They have further proposed that the defect in HCO_3^- secretion during secretin stimulation in patients with cystic fibrosis (CF) is at least partly due to lack of HCO_3^- uptake via NBCe1B [2].

The brain-type cotransporter NBCe1C, the C-terminal variant skipping exon 24, is mainly expressed in brain, but its physiological role remains to be established [3]. Homozygous inactivating mutations in NBCe1 cause proximal renal tubule acidosis (pRTA) associated with ocular abnormalities such as bandkeratopathy, cataract, and glaucoma. So far 12 homozygous NBCe1A mutations have been reported. They are 8 missense mutations (R298S, S427L, T485S, G486R, R510H, L522P, A799V and R881C) [28-32], two nonsense mutations (Q29X and W516X) [33, 34], and two frameshift mutations (2311 delA, S982NfsX4) [35, 36]. Functional analysis using different expression systems suggested that at least 50% reduction in the transport activity of NBCe1A would be necessary to induce the severe pRTA, defined as the reduction of blood HCO_3^- concentration to less than 13 mM [30, 31]. The close inspection of individual pRTA cases, however, revealed no tight relationship between the degree of NBCe1A inactivation and the severity of pRTA, suggesting that factor(s) other than the inactivation of transport function *per se* would be also involved. Indeed, several missense mutations such R298S, S427L, R510H, L522P, and R881C showed trafficking defects in the polarized Madin-Darby canine kidney (MDCK) cells [31, 37, 38]. Moreover, the NBCe1B mutants, corresponding to R510H, L522P, R881C, and

S982NfsX4 mutations in NBCe1A, showed almost no transport activities due to defective membrane expression in human embryonic kidney (HEK293) cells, which seems to be linked to the occurrence of migraine through the near total inactivation of NBCe1 activity in astrocytes [36]. Clinical Phenotypes of NBCe1 mutations are summarized in Table 1. As shown in Fig. 2, bicarbonate uptake into astrocytes via NBCe1 is though to suppress neuronal excitation by reducing the activity of pH-sensitive N-methyl D-aspartate receptor (NMDR).

Recently another NBCe1 mutation W516X was identified in a typical pRTA patient with ocular abnormalities, and mice carrying this mutation were produced [34]. I had a chance to examine the NBCe1 activity in isolated proximal tubules from these mice. As shown in Fig. 3a, the NBCe1 activity was modestly decreased in hetero mice ($NBCe1^{+/W516X}$) mice and markedly decreased in homo mice ($NBCe1^{W516X/W516X}$). The rates of HCO_3^- absorption ($JHCO_3^-$) from isolated renal proximal tubules were also moderately reduced in hetero mice and severely reduced in homo mice, as shown in Fig. 3b. In collaboration with Dr. Ishiguro in Nagoya University, I also examined the rates of fluid secretion into isolated pancreatic ducts from these mice. As shown in Fig. 4, the basal pancreatic duct fluid secretion was diminished and the forskolin-stimulated secretion was severely reduced in homo mice. These results confirmed the essential roles of NBCe1 in both renal proximal tubule bicarbonate absorption and pancreatic duct fluid secretion.

In addition to these naturally occurring mutations linked to pRTA and extrarenal manifestations, an extensive mutagenesis study revealed several amino acid residues of NBCe1 critical for the normal transport functions [39]. Furthermore, a C-terminal motif essential for the proper NBCe1 trafficking was also identified [40]. However, the

detailed structural basis of NBCe1-mediated Na^+-HCO_3^- cotransport across the plasma membrane is still largely unknown.

Besides its fundamental role as a major bicarbonate exit pathway, NBCe1A may also play an important role in the net sodium reabsorption process in renal proximal tubules. Approximately 60% of the NaCl filtered from glomerulus is reabsorbed in proximal tubules, and this process is facilitated by the coordinated operation of the apical Na^+/H^+ exchanger isoform 3 (NHE3) and the basolateral NBCe1A, with accompanying water absorption [41]. Notably, NHE3-deficient mice show hypotension, even after the transgenic rescue of intestinal absorptive defect [42]. Therefore, functional alterations in NBCe1A can be also theoretically linked to blood pressure variations. Indeed, NBCe1A in proximal tubules is one of target transporters that are stimulated by angiotensin II, a hormone implicated in blood pressure control at least partially by stimulating sodium reabsorption from proximal tubules [43, 44]. Moreover, spontaneously hypertension rats show the defective inhibition of NBCe1A activity by dopamine [45]. In the present study, I attempted to perform functional characterization of nonsynonymous single nucleotide polymorphisms (SNPs) in NBCe1A. Among 4 nonsynonymous SNPs that have been reported (http://www.ncbi.nlm.nih.gov/snp/), I revealed that only the K558R variant inactivates the transport function without impairing the trafficking behavior or the extracellular Na^+ affinity.

Methods

Construction of NBCe1A expressing constructs

cDNAs encoding human NBCe1A was subcloned into pcDNA3.1 as described [30, 31]. The QuikChange Site-Directed Mutagenesis kit (Stratagene) was used to introduce mutations. Sense primers used to introduce mutagenesis were 5'-GAGCTGAGGACATGTATGGGGAAAGGATCCATCATGCTTG-3' (for E122G), 5'-CTAAGAGTCTTCCATCCTATGACAAAAGAAAGAATATG-3' (for S356Y), 5'-CTTTATCTATGATGCTTTCAAGAGGATGATCAAGCTTGCAGATTAC-3' (for K558R), and 5'-GGAGGAAACCTCGTCGGGATCAACTGTAATTTTGTTCCTG-3' (for N640I). For GFP-tagged constructs, coding sequences of NBCe1A were subcloned into pcDNA3.1/NH2-terminal GFP-TOPO (both from Invitrogen). The complete cDNA sequence of each construct was verified by DNA sequencing.

Oocytes preparation

cRNAs were transcribed from the appropriately linearized templates with the mMESSAGE mMACHINE high-yield Capped RNA Transcription kit (Ambion). Oocytes were removed from *Xenopus laevis*, dissociated with collagenase as described [30, 31], and were injected with 50 nl of cRNA solution containing 5 ng of cRNA expressing each NBCe1A construct. Electrophysiological studies were performed 3 to 5 days after cRNA injection. To determine the electrophysiological activities of NBCe1A, I analyzed at least three different batches of oocytes, and the wild-type and SNP variants were analyzed on the same days.

Electrophysiological analysis

To determine the transport activity of NBCe1A, I analyzed at least three batches of oocytes from different *Xenopus*, and WT and mutants were analyzed on the same days. Nominally HCO_3^--free ND96 solution contained (in mM) 96 NaCl, 2 KCl, 1 $MgCl_2$, 1.8 $CaCl_2$, and 5 mM HEPES at a pH of 7.4. HCO_3^--containing solution was prepared by replacing 30 mM NaCl with 30 mM $NaHCO_3$ in ND96, and was equilibrated with 5% CO_2 in oxygen (pH 7.4). Electrophysiological studies were performed as described [30, 31]. In brief, an oocyte was placed in a perfusion chamber and superfused with ND96 solution at a rate of ~4 ml/min. To measure the NBCe1A-mediated current, a two-electrode voltage clamp method was used with a model CEZ-1200 dual-electrode voltage clamp amplifier (NIHON KOHDEN) connected to a Duo773 high input impedance differential electrometer (WPI), controlled by the Clampex module of pCLAMP software (Axon Instruments). I monitored the NBCe1A currents induced by solution changes from ND96 to HCO_3^--containing solution at a holding potential of –25 mV, because the baseline current was minimal at this voltage when oocytes were bathed in ND96 solution [30, 31]. In oocytes injected with H_2O, solution changes from ND96 to HCO_3^--containing solution did not induce any currents as described [30, 31, 35].

To determine the apparent Na^+ affinity of NBCe1A, extracellular Na^+ concentrations were sequentially reduced from 96 to 48, 24, 12 and 0 mM, while the NBCe1A currents were continuously monitored at a holding potential of –25 mV as reported [30]. The current at 0 mM Na^+ was subtracted from the raw data to obtain the corrected currents at the individual Na^+ concentrations. Damping Gauss Newton Method was used to fit data into the Michaelis-Menten equation as described [30].

Expression in cultured cells

MDCK and HEK293 cells were grown on culture dishes in Dulbecco's modified Eagles's medium supplemented with 10% fetal calf serum. These cells were transfected with plasmid expressing each NBCe1A construct with LipofectAMINE 2000 (Invitrogen). The same amounts of DNA (4 μg per well of 6-well dishes, or 24 μg per dish of 10-cm dishes) were transfected for the wild-type NBCe1A and the mutants. The cell pH measurement, immunoblotting or immnuofluorescence analyses were performed 48 hrs after transfection.

Cell pH measurements

HEPES-buffered solution contained (in mM) 127 NaCl, 5 KCl, 1.5 $CaCl_2$, 1 $MgCl_2$, 2 NaH_2PO_4, 1 Na_2SO_4, 25 HEPES, 5.5 glucose; adjusted to pH 7.4 by 1N NaOH. HCO_3^--Ringer solution contained (in mM) 115 NaCl, 5 KCl, 1.5 $CaCl_2$, 1 $MgCl_2$, 2 NaH_2PO_4, 1 Na_2SO_4, 25 $NaHCO_3$, 5.5 glucose; pH 7.4 equilibrated with 5% CO_2/95% O_2 gas. Na^+ was replaced by N-methyl-D-glucamine in Na^+-free HCO_3^--solution and Na^+-free HEPES-solution. HEK293 cells were grown on fibronectin-coated coverslips. Two days after transfection, cells were incubated with the pH dye acetoxymethylester of bis(carboxyethyl)carboxyfluorescein (BCECF/AM; Molecular Probes). Cell pH measurements were performed with a microscopic fluorescence photometry system (OSP-10; Olympus) as described [36]. The intracellular dye was alternatively excited at two wavelengths (440 and 490 nm), and emission was measured at a wavelength of 530 nm. NBCe1A activity in HEK293 cells was analyzed by monitoring Na^+- and HCO_3^--dependent cell pH recovery as described [36]. In brief, cells were first superfused with HEPES-buffered Ringer solution. Solution was exchanged to Na^+-free

HCO_3^--solution, which induced a marked intracellular acidification due to CO_2 entry. Thereafter, solution was exchanged to HCO_3^--Ringer solution containing 1 mM amiloride, which blocks the endogenous Na^+/H^+ exchange activity. The resultant Na^+- and HCO_3^--dependent cell pH recovery (dpH_i/dt) represents the NBCe1A activity [36]. In some experiments, cell pH recovery was induced by HCO_3^--Ringer solution containing both 1 mM amiloride and 0.5 mM 4, 4'-diisothiocyanatostilbene-2, 2'-disulphonic acid (DIDS, Sigma, an inhibitor of bicarbonate transporters). To examine the NBCe1A activity in the absence of HCO_3^-/CO_2, cell pH measurements were performed in HEPES-buffered solutions. In this case, cells were first superfused with HEPES-buffered Ringer solution. To induce an intracellular acidification, cells were superfused for 1~2 min with NH_4Cl-containing solution, which replaces 20 mM NaCl in HEPES-buffered Ringer solution with the equimolar amount of NH_4Cl. After cells were superfused with Na^+-free HEPES solution, solution was finally exchanged to HEPES-buffered Ringer solution containing 1 mM amiloride. These HEPES-buffered solutions were bubbled with 100% O_2 gas. The intrinsic cell buffer capacity (β_i) was measured with the NH_4Cl pulse method as described [30]. The relationship between cell pH and β_i was shown in Fig. 5. Total cell buffer capacity (β_T) in the HCO_3^--containing solution was equal to the sum of β_i and the HCO_3^- buffer capacity (β_{HCO3}-), and the HCO_3^--flux through NBCe1A was calculated as $dpH_i/dt \times \beta_T$. The calibration curve for cell pH was made as described [31]. In brief, cells were exposed to HEPES-buffered solution containing 120 mM K^+ and 10 μM nigericin. Solution pH was adjusted at the different levels (from 6.4 to 7.6) with 1N NaOH, whereas Na^+ concentration in solution was kept constant at 20 mM.

Cell surface biotinylation

Cell surface biotinylation in HEK293 cells was performed with the Pierce Cell Surface Protein Isolation Kit (Thermo Scientific) according to the manufacturer's protocol. In brief, cells, grown on 4 dishes of 10-cm culture dish, were washed with PBS, incubated with EZ-LINK Sulfo-NHS-SS-biotin for 30 min at 4 ^{o}C followed by the addition of a quenching solution. Cells were lysed with lysis buffer (500 μl) containing the Halt protease inhibitor cocktail kit. An aliquot (100 μl) of the lysate (total) was saved for Western blotting. The biotinylated NBCe1A was isolated with NeutrAvidin agarose gel, eluted by the sample buffer (400 μl) containing dithiothreitol, and subjected for immunoblotting as described [31]. In brief, after being dissolved in a sample-loading buffer that contained 2% SDS, the protein samples were separated by sodium dodecyl sulfate polyacrylamide gel electrophoresis on acrylamide minigels and transferred to a nitrocellulose membrane. After incubation in a blocking buffer, the membrane was treated with a diluted rabbit polyclonal anti-GFP antibody (Invitrogen) or a rabbit polyclonal anti-Na/K pump α1 antibody (Upstate Biotech) as described [36]. Thereafter, horseradish peroxidase-conjugated anti-rabbit IgG (BioRad) was used as the secondary antibody. The signal was detected by an ECL Plus system (Amersham).

Immunofluoresence

HEK293 cells or confluent MDCK cells were grown on fibronectin-coated coverslips. The confluent MDCK cells on coverslips were shown to retain the proper cell polarity, as evidenced by the basolateral distribution of Na/K pump and the formation of tight junctions [31, 38]. Moreover, the expression of NBCe1 was shown to be more efficient in this condition than when they were grown on permeable supports

[38]. The cells were fixed in 4% paraformaldehyde in PBS, permeabilized with 0.1% Triton X-100 (Sigma) in PBS, stained with the F-actin dye tetramethylrhodamine isothiocyanate-phalloidin (Sigma), and observed by a TCS SL laser-scanning confocal microscope (Leica) as described [31, 36]. To visualize the GFP-untagged NBCe1A constructs in MDCK cells, a rabbit polyclonal antibody against C-terminal region (amino acids 928 to 1035) of NBCe1 (Chemicon) was used as the primary antibody, and Alexa Fluor 488 goat anti-rabbit IgG (Molecular Probes) was used as the secondary antibody as described [31]. I performed at least 3 independent transfection studies examining at least 100 NBCe1A expressing cells in each case. The summary of experimental procedures are shown in Table 2.

Statistical analysis

The data were represented as mean $\pm$ SEM. Significant differences were determined by applying Student's t test or ANOVA with Bonferroni's correction, as appropriate. Statistical significance was set at $p < 0.05$.

Results

Functional analysis in Xenopus oocytes

Four nonsynonymous SNPs (E122G, S356Y, K558R, and N640I) within the SLC4A4 gene encoding variant NBCe1A transporters have been reported (http://www.ncbi.nlm.nih.gov/snp/) as shown in Fig. 6. Allele frequency is reported only for the K558R variant (0.014 in pilot.1.CEU population assembled by 1000 Genomes Project) and the N640I variant (0.013 in AGI_ASP population consisting of Caucasian and African-American females). The clinical phenotypes of carriers for these variants were not reported. To examine the effects of SNPs on NBCe1A function, I first performed the electrophysiological analysis in *Xenopus* oocytes using the GFP-untagged constructs, which have been used to characterize the electrogenic properties of NBCe1 [30, 31, 35, 46]. I monitored the outward currents induced by the solution exchange from ND96 solution to HCO_3^--containing solution at a holding potential of –25 mV, which reliably reflect the NBCe1A currents [30, 31, 35, 46]. As shown in Fig. 7a, the E122G, S356Y, and N640I variants had electrogenic activities comparable to that of wild-type NBCe1A. However, the K558R variant had a reduced activity ($p < 0.01$) corresponding to 47.0 $\pm$ 5.4% of that of wild-type NBCe1A.

Apparent Na^+ affinity

To clarify the effects of K558R variant on NBCe1A properties in more detail, I examined the apparent Na^+ affinity as described [30]. The current was continuously monitored at a holding potential of –25 mV, whereas extracellular Na^+ concentrations were changed sequentially from 96 mM to 48, 24, 12, and 0 mM. By subtracting the current at 0 mM Na^+ from raw data and fitting these data into the Michaelis-Menten

equation through nonlinear regression analysis, I obtained an individual curve for the wild-type and the K558R variant as shown in Fig. 7b. The calculated Km values of wild-type (31.7 $\pm$ 3.9 mM, n = 6) and K558R (29.6 $\pm$ 0.8 mM, n = 7) were not statically different, indicating that the reduced activity of K558R variant is not due to the reduction in apparent extracellular Na^+ affinity.

Intracellular expression in mammalian cells

Theoretically, NBCe1A mutations can reduce the overall transport function through the inactivation of individual transporter and/or the reduction in membrane expression. Furthermore, the previous studies suggested that the *Xenopus* oocytes expression system may not be ideal for the detection of trafficking abnormalities of NBCe1 mutants [30, 31, 36]. Therefore, I performed the confocal microscopic analysis to examine the intracellular expression of wild-type and the variants in mammalian cells using the GFP-tagged constructs.

In non-polarized HEK293 cells, the E122G, S356Y, K558R, and N640I variants showed the distinct membrane expression, which was very similar to that of wild-type NBCe1A (Fig. 8). These results indicate that these NBCe1A variants do not show abnormal trafficking in the non-polarized cells. On the other hand, the pRTA-related mutant R298S was reported to show the abnormal trafficking only in the polarized epithelium [30, 31, 37]. Accordingly, I also examined the intracellular expression in confluent MDCK cells, which have been thought to be useful for the analysis of NBCe1 trafficking in the polarized cells [31, 36-38]. As shown in Fig. 9a, the wild-type NBC1A showed the predominant basolateral membrane expression as reported [31]. As shown in Fig. 9b, the E122G, S356Y, K558R, and N640I variants also showed the predominant

basolateral membrane expression, which was indistinguishable from that of wild-type NBCe1A. To exclude any potential influence of the addition of GFP-tag, I also examined the intracellular expression of GFP-untagged constructs using the anti-NBCe1 antibody. As shown in Fig. 9c, all these constructs showed the predominant basolateral expression. These results indicate that none of SNPs variants show abnormal trafficking in the polarized mammalian cells.

Functional analysis in HEK293 cells

I next performed the functional analysis in HEK293 cells, which have been widely used to examine the transport function of NBCe1 [36, 47-49]. I used the GFP-tagged constructs, which have been shown to be useful in this system [50]. Solution exchange from HEPES-buffered solution to Na^+-free HCO_3^--solution rapidly reduced intracellular pH to around 6.8. As shown in Fig. 10a, cells transfected vector alone did not show cell pH recovery upon Na^+-addition as previously reported [36]. On the other hand, cells transfected with wild-type NBCe1A showed a prompt cell pH recovery upon Na^+-addition, and this cell pH recovery was completely inhibited by 0.5 mM DIDS as shown in Fig. 10b. The rates of cell pH recovery of wild-type were 0.67 $\pm$ 0.05 pH/min in the absence (n = 26) and -0.03 $\pm$ 0.02 pH/min (n = 6) in the presence of DIDS ($p < 0.01$), respectively. Cells transfected with the K558R variant also showed a prompt cell pH recovery upon Na^+-addition, but the rate of Na^+-dependent cell pH recovery was less than that of wild-type as shown in Fig. 10c. Consistent with the previous report [39], β_i (18.5 mM/pH) measured at the intracellular pH of 6.7 - 6.9 in HEK293 cells transfected by vector alone was unaffected by transfection with the wild-type NBC1A or the SNP variants. The initial cell pH values at which cells started Na^+-dependent pH recovery

were used to calculate β_{HCO_3}-. With these β_i and β_{HCO_3}- values, I obtained β_T values to calculate the HCO_3^- flux mediated by NBCe1A. As summarized in Fig. 10d, the E122G, S356Y, and N640I variants had transport activities comparable to that of wild-type. However, the K558R variant had a reduced transport activity ($p < 0.01$) corresponding to 40.8 $\pm$ 2.7% of that of wild-type NBCe1A. To exclude any potential influence of the addition of GFP-tag, I also performed functional analysis in HEK293 cells using the GFP-untagged constructs. As shown in Fig. 10e, I obtained the essentially similar results: only the K558R variant had a significantly reduced activity ($p < 0.05$) corresponding to 46.7$\pm$ 5.5% of that of wild-type NBCe1A.

The confocal microscopic analysis in HEK293 cells confirmed that the transfection efficiency of the GFP-tagged constructs (60 – 80%) was similar among wild-type and the SNP variants. To quantify the membrane expression levels of GFP-tagged wild-type and the variants, I performed the cell-surface biotinylation Western blotting. As shown in Fig. 11, all the variants showed the similar membrane expression as the wild-type NBCe1A. They also showed the similar whole cell expression as the wild-type NBCe1. These results indicate that only the K558R variant has a reduced transport activity, and that this reduction is not associated with any trafficking abnormalities.

In a separate set of experiments performed with HEPES-buffered solutions, I finally examined the HCO_3^--dependency of NBCe1A activity in HEK293 cells. As shown in Fig. 12, GFP-tagged wild-type NBCe1A showed a slow cell pH recovery even in the absence of HCO_3^-/CO_2. The rates of cell pH recovery were 0.13 $\pm$ 0.02 pH/min for wild-type ($n = 10$) and 0.02 $\pm$ 0.01 pH/min ($n = 8$) for vector ($p < 0.01$), respectively. I confirmed that 0.5 mM DIDS completely inhibited the slow cell pH recovery by wild-type ($n = 5$). The NBCe1A-mediated base flux in the absence of HCO_3^-/CO_2

calculated by the β_i value (18.5 mM/pH) and the rate of cell pH recovery (0.13 pH/min) was 2.4 $\pm$ 0.2 mM/min (n = 10). This value corresponded to only 11.1% of the NBCe1A-mediated HCO_3^- flux (21.7 $\pm$ 1.7 mM/min, n = 26) calculated by the β_T value (32.6 mM/pH) and the rate of cell pH recovery (0.67 pH/min) in the presence of HCO_3^-/CO_2. The absolute dependence on Na^+, the inhibition by DIDS, and the very low affinity to OH^-, if any, shown in this study were consistent with the properties of NBCe1A activity in HEK293 cells [47].

Discussion

In the present study I tried to perform functional characterization of the 4 nonsynonymous SNPs, E122G, S356Y, K558R, and N640I in NBCe1A. Because NBCe1 mutations are known to display variable trafficking behaviors depending on the expression systems [30, 31, 37, 38], I used several different approaches to clarify the effects of SNP variants. According to the topology models [49, 51], NBCe1 is presumed to have 13 or 14 transmembrane segments (TMs). Both models predict the E122G and S356Y variants in the N-terminal cytoplasmic region, the K558R variant in near the extracellular end of TM5, and the N640I variant in the extracellular loop between TM5 and TM6. Functional analysis in *Xenopus* oocytes revealed that while the K558R variant had a significantly reduced transport activity corresponding to 47% of the wild-type activity, the remaining variants E122G, S356Y and N640I did not change the NBCe1A activity. Apparent Na^+ affinity of K558R was not different from that of wild-type, indicating that the functional reduction of K558R variant is not due to the reduction in Na^+ affinity. Immunohistological analyses in HEK293 cells and MDCK cells indicated that none of these SNPs changed the trafficking behaviors of NBCe1A. Functional analysis in HEK293 cells also revealed that only the K558R variant had a reduced transport activity, corresponding to 41 - 47% of the wild-type activity. Furthermore, all of the variants had surface expression comparable to that of wild-type NBCe1 in HEK293 cells. From these results I conclude that while the K558R variant significantly reduces the NBCe1A activity without changing the trafficking behavior, the remaining 3 SNPs do not change the NBCe1A properties at all.

Consistent with the previous reports [36, 47-49], our functional analysis in HEK293 cells confirmed the absolute dependence of NBCe1 activity on Na^+. On the

other hand, I observed a small transport activity of NBCe1A even in the absence of HCO_3^-/CO_2, which corresponds to only 11% of the NBCe1A activity in the presence of HCO_3^-/CO_2. At present, I cannot definitely determine whether this small residual NBCe1A activity in the absence of HCO_3^-/CO_2 reflects the very low NBCe1A affinity for OH^- [47], or the transport of endogenous HCO_3^- metabolically produced by the cells [52].

The significant functional reduction by the K558R variant is consistent with the view that most of the missense residues causing pRTA lie deep in TMs, where they perform important structural roles [49]. The previous finding that an artificial mutant K558Q had a significantly reduced transport activity corresponding to 53% of that of wild-type [39] further supports the importance of K558. On the other hand, K558, K559 and K562 may constitute the ^{558}KKMIK motif, which may represent one of the putative binding sites for 4, 4'-diisothiocyanatostilbene-2, 2'-disulphonic acid (DIDS) [51]. For example, the ^{558}RRMIR mutant had a slightly higher DIDS binding affinity, while ^{558}NNMIN mutant had a markedly reduced DIDS binding affinity. However, these mutants had HCO_3^- slope conductance comparable to that of wild-type in *Xenopus* oocytes. From these and other results, Lu and Boron concluded that ^{558}KKMIK motif is important for the reversible and irreversible interactions with DIDS, but not essential for the electrogenic transport activity of NBCe1A [51]. I speculate that the effect of single amino acid substitution of K558 is different from the simultaneous substitutions of K558, K559 and K562. The significant functional reduction caused by the amino acid substitutions both with (K558Q) or without (K558R) charge alterations rather support a critical role of K558 in the overall NBCe1 transport. It should be mentioned, however, that the amino acid substitutions of NBCe1 by different classes of amino acids would

not necessarily induce the similar functional effects. For example, the pRTA-related mutant L522P is predominantly retained in the cytoplasmic region and shows almost no functional activity in mammalian cells [31]. On the other hand, the artificial mutant L522C is properly processed to the plasma membrane and shows a significant activity corresponding to approximately 70% of the wild-type activity in HEK293 cells [49].

Based on the structural similarity in SLC4 bicarbonate transporters and the NBCe1A mutagenesis analysis, Chang et al. previously proposed that E91 is predicted to hydrogen-bound with R298, thereby constituting an ion transport pathway together with R86 and E92 [53]. Because E122G does not affect the NBCe1A activity, E122 may not be directly involved in this functionally important domain proposed by Chang et al. [53]. The residues near N640 in the extracellular loop have not been extensively analyzed. Only an artificial mutant D647R, predicted to line in the entry of TM6, was shown to markedly reduce the NBCe1 function [39].

Homozygous inactivating mutations in NBCe1 cause pRTA associated with ocular abnormalities and short stature. Functional analyses using the different expression systems have shown that as much as 50% reductions in NBCe1A activity can induce these renal and extra renal phenotypes [15, 28-33, 35]. For example, T485S and G486R do not reach the plasma membrane in *Xenopus* oocytes. However, they show the proper membrane expression and have reduced transport activities corresponding to approximately 50% of that of wild-type in mammalian cells [30, 31]. These results strongly suggest that the K558R variant, which reduces the NBCe1A activity by at least 50%, should lead to the clinically apparent phenotypes, if present in the homozygous status, though such a pRTA patient has not been found yet. At present, the estimated population frequency of pRTA due to NBCe1 mutations is unknown. However, the

severe acidemia found in this disease is expected to impair reproductive fitness. Accordingly, K558R can be subject to purifying selection, which may potentially explain the rare allele frequency (0.014) of this variant.

The situation for the heterozygous status of K558R variant may be different from that for the homozygous status. Haploinsufficiency of NBCe1 in mice is associated with mild acidemia [54]. However, heterozygous human mutations in NBCe1 have not been linked to pRTA, probably due to much higher compensatory ability of renal distal tubules in humans [36]. Nevertheless, 50 - 60% reduction in NBCe1A activity by the K558R variant should have a substantial effect on the overall sodium handling by the kidney, even in the heterozygous status. Notably, rare heterozygous mutations in renal salt handling genes such as *SCL12A3*, *SLC12A1*, and *KCNJ1* have been shown to result in the lower blood pressure [55]. In fact, the mean long-term systolic blood pressure among mutation carriers were found be 6.3 mmHg lower than the mean of the cohort [55]. In view of the large capacity of proximal tubules to reabsorb sodium, it will be interesting to examine in the future studies whether the heterozygous status of K558R variant is also linked to health benefit through the reduction of blood pressure. On the other hand, Kao et al. recently found that NBCe1, like Cl^-/HCO_3^- exchanger AE1, is predominantly a homodimer that is composed of functionally active monomers [48].I have recently shown that the heterozygous S982NfsX4 mutation, which retains in the endoplasmic reticulum, causes migraine and normal-tension glaucoma through the hetero-oligomer formation with wild-type NBCe1 [36]. However, the K558R variant is quite unlikely to have such a dominant negative effect, because it shows the normal trafficking behavior in the mammalian cells.

In summary, I performed functional characterization of the 4 nonsynonymous

SNPs, E122G, S356Y, K558R, and N640I in NBCe1A. The results indicate that only the K558R variant inactivates the NBCe1 function without changing the apparent Na^+ affinity or the membrane trafficking behavior.

Acknowledgment

This study was supported in part by grants from the Ministry of Education, Culture, Sports, Science and Technology of Japan.

Table 1. Clinical Phenotypes of NBCe1 mutations.

Mutations	Gender	Blood HCO_3^- (mM) normal value = 24	Short stature	Glaucoma	membrane expression (NBCe1B)	Migraine	Migraine phenotypes
Q29X	F	9.4	Yes	Yes	Yes	No	
R298S	F	8	Yes	Yes	Yes	No	
S427L	F	11	Yes	Yes	Yes	No	
T485S	M	13	Yes	No	Yes	No	
G486R	F	10	Yes	No	Yes	No	
A779V	F	6.3	Yes	Yes	Yes	No	
R510H	F	5	Yes	Yes	No	Yes	MO
L522P	M	Not reported	Yes	Yes	No	Yes	Hemiplegia Ataxia
Δ2311A	M	13.2	Yes	Yes	No	Yes	MA
R881C	F	10.6	Yes	Yes	No	Yes	MO
Δ65bp III:3	F	17.3	No	Yes	No	Yes	Hemiplegia
Δ65bp III:5	F	14.8	No	Yes	No	Yes	Hemiplegia Stupor

MO: Migraine with aura, MA: migraine with aura.

Table 2. Summary of experimental procedures.

Cell types	Constructs	Types of Experiments
Xenopus Oocyte	GFP-untagged	1.NBCe1 currents 2.Na^+-affinity
MDCK cell (polarized cell)	GFP-tagged/-untagged	1.Intracellular localization
HEK cell (non-polarized cell)	GFP-tagged/-untagged	1.Intracellular localization 2.NBCe1 transport activity 3.cell surface expression(biotinylation western)

References

1. Romero MF, Boron WF: Electrogenic Na^+/HCO_3^- cotransporters: cloning and physiology. *Annu Rev Physiol* 61:699-723, 1999
2. Abuladze N, Song M, Pushkin A, Newman D, Lee I, Nicholas S, Kurtz I: Structural organization of the human NBC1 gene: kNBC1 is transcribed from an alternative promoter in intron 3. *Gene* 251:109-122, 2000
3. Bevensee MO, Schmitt BM, Choi I, Romero MF, Boron WF: An electrogenic Na^+-HCO_3^- cotransporter (NBC) with a novel COOH-terminus, cloned from rat brain. *Am J Physiol Cell Physiol* 278:C1200-1211, 2000
4. Romero MF, Hediger MA, Boulpaep EL, Boron WF: Expression cloning and characterization of a renal electrogenic Na^+/HCO_3^- cotransporter. *Nature* 387:409-413, 1997
5. Abuladze N, Lee I, Newman D, Hwang J, Boorer K, Pushkin A, Kurtz I: Molecular cloning, chromosomal localization, tissue distribution, and functional expression of the human pancreatic sodium bicarbonate cotransporter. *J Biol Chem* 273:17689-17695, 1998
6. Alper SL: Genetic diseases of acid-base transporters. *Annu Rev Physiol* 64:899-923, 2002
7. Boron WF, Boulpaep EL: Intracellular pH regulation in the renal proximal tubule of the salamander. Basolateral HCO_3^- transport. *J Gen Physiol* 81:53-94, 1983
8. Yoshitomi K, Burckhardt BC, Fromter E: Rheogenic sodium-bicarbonate cotransport in the peritubular cell membrane of rat renal proximal tubule. *Pflugers Arch* 405:360-366, 1985

9. Alpern RJ: Mechanism of basolateral membrane $H^+/OH^-/HCO_3^-$ transport in the rat proximal convoluted tubule. A sodium-coupled electrogenic process. *J Gen Physiol* 86:613-636, 1985

10. Soleimani M, Aronson PS: Ionic mechanism of Na^+-HCO_3^- cotransport in rabbit renal basolateral membrane vesicles. *J Biol Chem* 264:18302-18308, 1989

11. Seki G, Coppola S, Yoshitomi K, Burckhardt BC, Samarzija I, Muller-Berger S, Fromter E: On the mechanism of bicarbonate exit from renal proximal tubular cells. *Kidney Int* 49:1671-1677, 1996

12. Ishiguro H, Steward MC, Wilson RW, Case RM: Bicarbonate secretion in interlobular ducts from guinea-pig pancreas. *J Physiol* 495 (Pt 1):179-191, 1996

13. Ishiguro H, Steward MC, Lindsay AR, Case RM: Accumulation of intracellular HCO_3^- by Na^+-HCO_3^- cotransport in interlobular ducts from guinea-pig pancreas. *J Physiol* 495 (Pt 1):169-178, 1996

14. Marino CR, Jeanes V, Boron WF, Schmitt BM: Expression and distribution of the Na^+-HCO_3^- cotransporter in human pancreas. *Am J Physiol* 277:G487-494, 1999

15. Satoh H, Moriyama N, Hara C, Yamada H, Horita S, Kunimi M, Tsukamoto K, Iso ON, Inatomi J, Kawakami H, Kudo A, Endou H, Igarashi T, Goto A, Fujita T, Seki G: Localization of Na^+-HCO_3^- cotransporter (NBC-1) variants in rat and human pancreas. *Am J Physiol Cell Physiol* 284:C729-737, 2003

16. Roussa E, Nastainczyk W, Thevenod F: Differential expression of electrogenic NBC1 (SLC4A4) variants in rat kidney and pancreas. *Biochem Biophys Res Commun* 314:382-389, 2004

17. Jacob P, Christiani S, Rossmann H, Lamprecht G, Vieillard-Baron D, Muller R,

Gregor M, Seidler U: Role of Na^+HCO_3- cotransporter NBC1, Na^+/H^+ exchanger NHE1, and carbonic anhydrase in rabbit duodenal bicarbonate secretion. *Gastroenterology* 119:406-419, 2000

18. Bachmann O, Rossmann H, Berger UV, Colledge WH, Ratcliff R, Evans MJ, Gregor M, Seidler U: cAMP-mediated regulation of murine intestinal/pancreatic Na^+/HCO_3^- cotransporter subtype pNBC1. *Am J Physiol Gastrointest Liver Physiol* 284:G37-45, 2003

19. Usui T, Hara M, Satoh H, Moriyama N, Kagaya H, Amano S, Oshika T, Ishii Y, Ibaraki N, Hara C, Kunimi M, Noiri E, Tsukamoto K, Inatomi J, Kawakami H, Endou H, Igarashi T, Goto A, Fujita T, Araie M, Seki G: Molecular basis of ocular abnormalities associated with proximal renal tubular acidosis. *J Clin Invest* 108:107-115, 2001

20. Bok D, Schibler MJ, Pushkin A, Sassani P, Abuladze N, Naser Z, Kurtz I: Immunolocalization of electrogenic sodium-bicarbonate cotransporters pNBC1 and kNBC1 in the rat eye. *Am J Physiol Renal Physiol* 281:F920-935, 2001

21. Chesler M: Regulation and modulation of pH in the brain. *Physiol Rev* 83:1183-1221, 2003

22. Brune T, Fetzer S, Backus KH, Deitmer JW: Evidence for electrogenic sodium-bicarbonate cotransport in cultured rat cerebellar astrocytes. *Pflugers Arch* 429:64-71, 1994

23. Schmitt BM, Berger UV, Douglas RM, Bevensee MO, Hediger MA, Haddad GG, Boron WF: Na/HCO_3 cotransporters in rat brain: expression in glia, neurons, and choroid plexus. *J Neurosci* 20:6839-6848, 2000

24. Goyal S, Vanden Heuvel G, Aronson PS: Renal expression of novel Na^+/H^+

exchanger isoform NHE8. *Am J Physiol Renal Physiol* 284:F467-473, 2003

25. Coppola S, Fromter E: An electrophysiological study of angiotensin II regulation of Na-HCO_3 cotransport and K conductance in renal proximal tubules. I. Effect of picomolar concentrations. *Pflugers Arch* 427:143-150, 1994

26. Shcheynikov N, Wang Y, Park M, Ko SB, Dorwart M, Naruse S, Thomas PJ, Muallem S: Coupling modes and stoichiometry of Cl^-/HCO_3^- exchange by slc26a3 and slc26a6. *J Gen Physiol* 127:511-524, 2006

27. Whitcomb DC, Ermentrout GB: A mathematical model of the pancreatic duct cell generating high bicarbonate concentrations in pancreatic juice. *Pancreas* 29:e30-40, 2004

28. Igarashi T, Inatomi J, Sekine T, Cha SH, Kanai Y, Kunimi M, Tsukamoto K, Satoh H, Shimadzu M, Tozawa F, Mori T, Shiobara M, Seki G, Endou H: Mutations in SLC4A4 cause permanent isolated proximal renal tubular acidosis with ocular abnormalities. *Nat Genet* 23:264-266, 1999

29. Dinour D, Chang MH, Satoh J, Smith BL, Angle N, Knecht A, Serban I, Holtzman EJ, Romero MF: A novel missense mutation in the sodium bicarbonate cotransporter (NBCe1/SLC4A4) causes proximal tubular acidosis and glaucoma through ion transport defects. *J Biol Chem* 279:52238-52246, 2004

30. Horita S, Yamada H, Inatomi J, Moriyama N, Sekine T, Igarashi T, Endo Y, Dasouki M, Ekim M, Al-Gazali L, Shimadzu M, Seki G, Fujita T: Functional analysis of NBC1 mutants associated with proximal renal tubular acidosis and ocular abnormalities. *J Am Soc Nephrol* 16:2270-2278, 2005

31. Suzuki M, Vaisbich MH, Yamada H, Horita S, Li Y, Sekine T, Moriyama N,

Igarashi T, Endo Y, Cardoso TP, de Sa LC, Koch VH, Seki G, Fujita T: Functional analysis of a novel missense NBC1 mutation and of other mutations causing proximal renal tubular acidosis. *Pflugers Arch* 455:583-593, 2008

32. Demirci FY, Chang MH, Mah TS, Romero MF, Gorin MB: Proximal renal tubular acidosis and ocular pathology: a novel missense mutation in the gene (SLC4A4) for sodium bicarbonate cotransporter protein (NBCe1). *Mol Vis* 12:324-330, 2006

33. Igarashi T, Inatomi J, Sekine T, Seki G, Shimadzu M, Tozawa F, Takeshima Y, Takumi T, Takahashi T, Yoshikawa N, Nakamura H, Endou H: Novel nonsense mutation in the Na^+/HCO_3^- cotransporter gene (SLC4A4) in a patient with permanent isolated proximal renal tubular acidosis and bilateral glaucoma. *J Am Soc Nephrol* 12:713-718, 2001

34. Lo YF, Yang SS, Seki G, Yamada H, Horita S, Yamazaki O, Fujita T, Usui T, Tsai JD, Yu IS, Lin SW, Lin SS: Severe metabolic acidosis causes early lethality in NBC1 W516X knock-in mice as a model of human isolated proximal renal tubular acidosis. *Kidney Int* In press.

35. Inatomi J, Horita S, Braverman N, Sekine T, Yamada H, Suzuki Y, Kawahara K, Moriyama N, Kudo A, Kawakami H, Shimadzu M, Endou H, Fujita T, Seki G, Igarashi T: Mutational and functional analysis of SLC4A4 in a patient with proximal renal tubular acidosis. *Pflugers Arch* 448:438-444, 2004

36. Suzuki M, Van Paesschen W, Stalmans I, Horita S, Yamada H, Bergmans BA, Legius E, Riant F, De Jonghe P, Li Y, Sekine T, Igarashi T, Fujimoto I, Mikoshiba K, Shimadzu M, Shiohara M, Braverman N, Al-Gazali L, Fujita T, Seki G: Defective membrane expression of the Na^+-HCO_3^- cotransporter NBCe1

is associated with familial migraine. *Proc Natl Acad Sci U S A* 107:15963-15968, 2010

37. Li HC, Szigligeti P, Worrell RT, Matthews JB, Conforti L, Soleimani M: Missense mutations in Na^+:HCO_3^- cotransporter NBC1 show abnormal trafficking in polarized kidney cells: a basis of proximal renal tubular acidosis. *Am J Physiol Renal Physiol* 289:F61-71, 2005

38. Toye AM, Parker MD, Daly CM, Lu J, Virkki LV, Pelletier MF, Boron WF: The human NBCe1-A mutant R881C, associated with proximal renal tubular acidosis, retains function but is mistargeted in polarized renal epithelia. *Am J Physiol Cell Physiol* 291:C788-801, 2006

39. Abuladze N, Azimov R, Newman D, Sassani P, Liu W, Tatishchev S, Pushkin A, Kurtz I: Critical amino acid residues involved in the electrogenic sodium-bicarbonate cotransporter kNBC1-mediated transport. *J Physiol* 565:717-730, 2005

40. Li HC, Worrell RT, Matthews JB, Husseinzadeh H, Neumeier L, Petrovic S, Conforti L, Soleimani M: Identification of a carboxyl-terminal motif essential for the targeting of Na^+-HCO_3^- cotransporter NBC1 to the basolateral membrane. *J Biol Chem* 279:43190-43197, 2004

41. Wang T, Yang CL, Abbiati T, Schultheis PJ, Shull GE, Giebisch G, Aronson PS: Mechanism of proximal tubule bicarbonate absorption in NHE3 null mice. *Am J Physiol* 277:F298-302, 1999

42. Woo AL, Noonan WT, Schultheis PJ, Neumann JC, Manning PA, Lorenz JN, Shull GE: Renal function in NHE3-deficient mice with transgenic rescue of small intestinal absorptive defect. *Am J Physiol Renal Physiol* 284:F1190-1198,

2003

43. Crowley SD, Gurley SB, Herrera MJ, Ruiz P, Griffiths R, Kumar AP, Kim HS, Smithies O, Le TH, Coffman TM: Angiotensin II causes hypertension and cardiac hypertrophy through its receptors in the kidney. *Proc Natl Acad Sci U S A* 103:17985-17990, 2006

44. Li Y, Yamada H, Kita Y, Kunimi M, Horita S, Suzuki M, Endo Y, Shimizu T, Seki G, Fujita T: Roles of ERK and cPLA2 in the angiotensin II-mediated biphasic regulation of Na^+-HCO_3^- transport. *J Am Soc Nephrol* 19:252-259, 2008

45. Kunimi M, Seki G, Hara C, Taniguchi S, Uwatoko S, Goto A, Kimura S, Fujita T: Dopamine inhibits renal Na^+:HCO_3^- cotransporter in rabbits and normotensive rats but not in spontaneously hypertensive rats. *Kidney Int* 57:534-543, 2000

46. Shirakabe K, Priori G, Yamada H, Ando H, Horita S, Fujita T, Fujimoto I, Mizutani A, Seki G, Mikoshiba K: IRBIT, an inositol 1,4,5-trisphosphate receptor-binding protein, specifically binds to and activates pancreas-type Na^+/HCO_3^- cotransporter 1 (pNBC1). *Proc Natl Acad Sci U S A* 103:9542-9547, 2006

47. Amlal H, Wang Z, Burnham C, Soleimani M: Functional characterization of a cloned human kidney Na^+:HCO_3^- cotransporter. *J Biol Chem* 273:16810-16815, 1998

48. Kao L, Sassani P, Azimov R, Pushkin A, Abuladze N, Peti-Peterdi J, Liu W, Newman D, Kurtz I: Oligomeric structure and minimal functional unit of the electrogenic sodium bicarbonate cotransporter NBCe1-A. *J Biol Chem* 283:26782-26794, 2008

49. Zhu Q, Kao L, Azimov R, Newman D, Liu W, Pushkin A, Abuladze N, Kurtz I:

Topological location and structural importance of the NBCe1-A residues mutated in proximal renal tubular acidosis. *J Biol Chem* 285:13416-13426, 2010

50. Bachmann O, Franke K, Yu H, Riederer B, Li HC, Soleimani M, Manns MP, Seidler U: cAMP-dependent and cholinergic regulation of the electrogenic intestinal/pancreatic Na^+/HCO_3^- cotransporter pNBC1 in human embryonic kidney (HEK293) cells. *BMC Cell Biol* 9:70, 2008

51. Lu J, Boron WF: Reversible and irreversible interactions of DIDS with the human electrogenic Na/HCO_3 cotransporter NBCe1-A: role of lysines in the KKMIK motif of TM5. *Am J Physiol Cell Physiol* 292:C1787-1798, 2007

52. Krapf R, Alpern RJ, Rector FC, Jr., Berry CA: Basolateral membrane Na/base cotransport is dependent on CO_2/HCO_3 in the proximal convoluted tubule. *J Gen Physiol* 90:833-853, 1987

53. Chang MH, DiPiero J, Sonnichsen FD, Romero MF: Entry to "formula tunnel" revealed by SLC4A4 human mutation and structural model. *J Biol Chem* 283:18402-18410, 2008

54. Gawenis LR, Bradford EM, Prasad V, Lorenz JN, Simpson JE, Clarke LL, Woo AL, Grisham C, Sanford LP, Doetschman T, Miller ML, Shull GE: Colonic anion secretory defects and metabolic acidosis in mice lacking the NBC1 Na^+/HCO_3^- cotransporter. *J Biol Chem* 282:9042-9052, 2007

55. Ji W, Foo JN, O'Roak BJ, Zhao H, Larson MG, Simon DB, Newton-Cheh C, State MW, Levy D, Lifton RP: Rare independent mutations in renal salt handling genes contribute to blood pressure variation. *Nat Genet* 40:592-599, 2008

Figure legends

Fig. 1 A schematic of the modes and directions of operation of the Na^+-HCO_3^- cotransporter (NBCe1) in kidney proximal tubule cells and pancreatic duct cells. **(a)** In renal proximal tubule, the Na^+/H^+ exchangers (NHE3 and/or NHE8) and the proton pump are localized in the apical membrane. The basolateral Na^+-HCO_3^- cotransporter (NBCe1A) works in efflux mode presumably with a stoichiometry of 3 HCO_3^- per 1Na^+. **(b)** In the pancreas, Cl^-/HCO_3^- exchangers (AE and/or SLC26A) and cystic fibrosis transmembrane conductance regulator (CFTR) are localized in the apical membrane. The basolateral Na^+-HCO_3^- cotransporter (NBCe1B) works in the influx mode presumably with a stoichiometry of 2 HCO_3^- per 1Na^+.

Fig. 2 Role of NBCe1 in regulation of neuronal excitability. FHM: familial hemiplegic migraine, CACNA1A: α1 subunit of voltage-gated neuronal $Ca_v2.1$ calcium channels, ATP1A2: α2 subunit of Na^+/K^+ pump, SCN1A: neuronal voltage-gated sodium channel $Na_v1.1$, NMDAR: N-methyl D-aspartate receptor. Neuronal excitation leads to the increase in extracellular K^+ concentration, which depolarizes cell membrane potentials of astrocytes. This depolarization facilitates HCO_3^- uptake into astrocytes through the electrogenic NBCe1. The resultant decrease in extracellular pH may suppress the activity of pH-sensitive NMDR.

Fig. 3 Role of NBCe1 in renal proximal tubule bicarbonate absorption. **(a)** Summary data for NBCe1 activity in isolated renal proximal tubules from $NBCe1^{+/+}$ (n=8),

$NBCe1^{+/W516X}$ (n=12) and $NBCe1^{W516X/W516X}$ (n=7) mice. NBCe1 activity was calculated from the rates of cell pH changes in response to bath of HCO_3^- reduction. * P<0.01 versus $NBCe1^{+/+}$ mice, $^{\#}$P<0.01 versus $NBCe1^{+/W516X}$ mice. **(b)** Summary data for the rates of HCO_3^- absorption ($JHCO_3^-$) obtained from $NBCe1^{+/+}$ (n = 21), $NBCe1^{+/W516X}$ (n = 13) and $NBCe1^{W516X/W516X}$ (n = 13) mice. $JHCO_3^-$ was measured by the stop-flow microfluorescence method [44]. *P < 0.01 versus $NBCe1^{+/+}$ mice, $^{\#}$P < 0.01 versus $NBCe1^{+/W516X}$ mice.

Fig. 4 Basal and forskolin-stimulated fluid secretion in sealed interlobular pancreatic ducts. Sealed interlobular pancreatic ducts isolated from wild-type (WT) and $NBC1^{W516X/W516X}$ mice were superfused with the standard HCO_3^--CO_2-buffered solution, and forskolin (1μM) was added to the bath. **(a)** and **(b)**: time course of fluid secretory rate in WT (n=3) and $NBC1^{W516X/W516X}$ ducts (n=5), respectively.

Fig. 5 The relationship between cell pH and β_i in HEK293 cells transfected with vector. The NH_4Cl pulse method was used, and β_i measured at cell pH of 6.7 – 6.9 was 18.5 $\pm$ 0.9 mM/pH (n = 10). The line represents the linear regression, where the coefficient of determination (R^2) is 0.54

Fig. 6 Topological model of NBCe1A according to the model for AE1 [51]. Red squares show the localization of SNP variants E122G (1), S356Y (2), K558R (3), and N640I (4). Blue circles show the localization of pRTA-related mutations Q29X (1), R298S (2), S427L (3), T485S (4), G486R (5), R510H (6), W516X (7), L522P (8), 2311 delA (9), A799V (10), R881C (11), and S982NfsX4 (12). The

dashed lines represent the specific regions of NBCe1B or NBCe1C, and the N and C denote the N- and C-terminus, respectively

Fig. 7 Functional analysis of SNP variants in *Xenopus* oocytes. **a** Summary of NBCe1 currents elicited by solution change from ND96 to HCO_3^--containing solution. **p < 0.01 vs wild-type (WT). Numbers of observations are 19 (WT), 10 (E122G), 10 (S356Y), 16 (K558R), and 10 (N640I). **b** Apparent Na^+ affinity for WT and K558R, determined by current monitoring during sequential reduction of extracellular Na^+ concentrations. Damping Gauss Newton Method was used to fit data into the Michaelis-Menten equation. Numbers of observation are six for WT and seven for K558R

Fig. 8 Intracellular localization of wild-type (WT) and SNP variants in HEK293 cells. GFP-tagged NBCe1A constructs are shown as green color. Only front views are shown. Note the predominant membrane expression of WT and SNPs. Bar indicates 10 μm

Fig. 9 Intracellular localization in MDCK cells. a. Expression of GFP-tagged wild-type NBCe1A (WT) is shown as green, and actin as red. XY indicates front view, and XZ side view. Note the predominant basolateral expression of NBCe1A. Bars indicate 10 μm. **b** Expression of GFP-tagged SNP variants. Note the similar basolateral expression of SNP variants. Details as in Fig. 9a. **c** Expression of GFP-untagged constructs detected by the anti-NBCe1 antibody. Details as in Fig. 9a

Fig. 10 Functional analysis in HEK293 cells in the presence of HCO_3^-/CO_2. **a-c** Original traces for cells transfected with vector (a), WT (b), and K558R (c) are shown. Note the absence of cell pH recovery in vector, the prompt cell pH recovery in WT that was completely inhibited by DIDS (0.5 mM), and the lower rate of cell pH recovery in K558R than in WT. AML: amiloride (1 mM). **d** Summary data for NBCe1-mediated HCO_3^- fluxes by the GFP-tagged constructs. Cont: cells transfected vector alone. **p<0.01 vs. WT. Numbers of observation are 26 (WT), 9 (E122G), 9 (S356Y), 22 (K558R), 21 (N640I), and 12 (Cont). **e** Summary data for NBCe1-mediated HCO_3^- fluxes by the GFP-untagged constructs. *p<0.05 vs. WT. Numbers of observation are 14 (WT), 10 (E122G), 7 (S356Y), 12 (K558R), 11 (N640I), and 9 (Cont)

Fig. 11 Cell surface expression of NBCe1A. Blots with the anti-GFP antibody in biotinylated (2 μl per lane) and total fractions (15 μl per lane) are shown. Equal protein loading in biotinylated fractions is confirmed by blots with anti-Na/K pump. A representative blot from 3 independent experiments is shown

Fig. 12 Functional analysis in HEK293 cells in the absence of HCO_3^-/CO_2. Cells were acidified by the NH_4Cl (20 mM) pulse. Note that the re-addition of Na^+ induces a slow cell pH recovery in cells transfected with WT. AML: amiloride (1 mM)

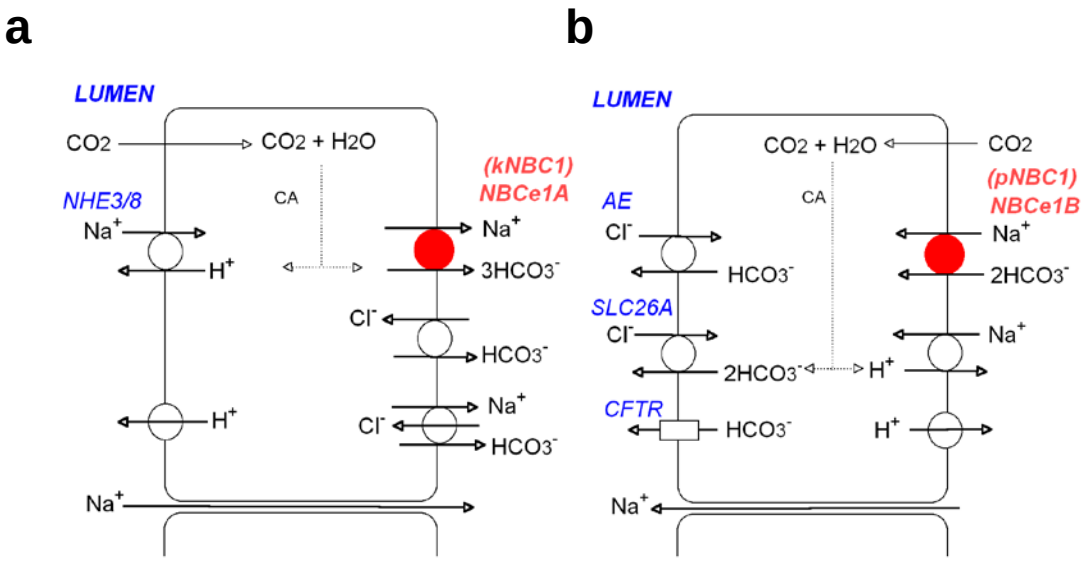
a
b
LUMEN
CO2
CO2 + H2O
CA
(kNBC1)
NBCe1A
NHE3/8
Na+
H+
3HCO3-
Cl-
HCO3-
LUMEN
CO2 + H2O
CO2
(pNBC1)
NBCe1B
AE
SLC26A
CFTR
2HCO3-

Fig. 1

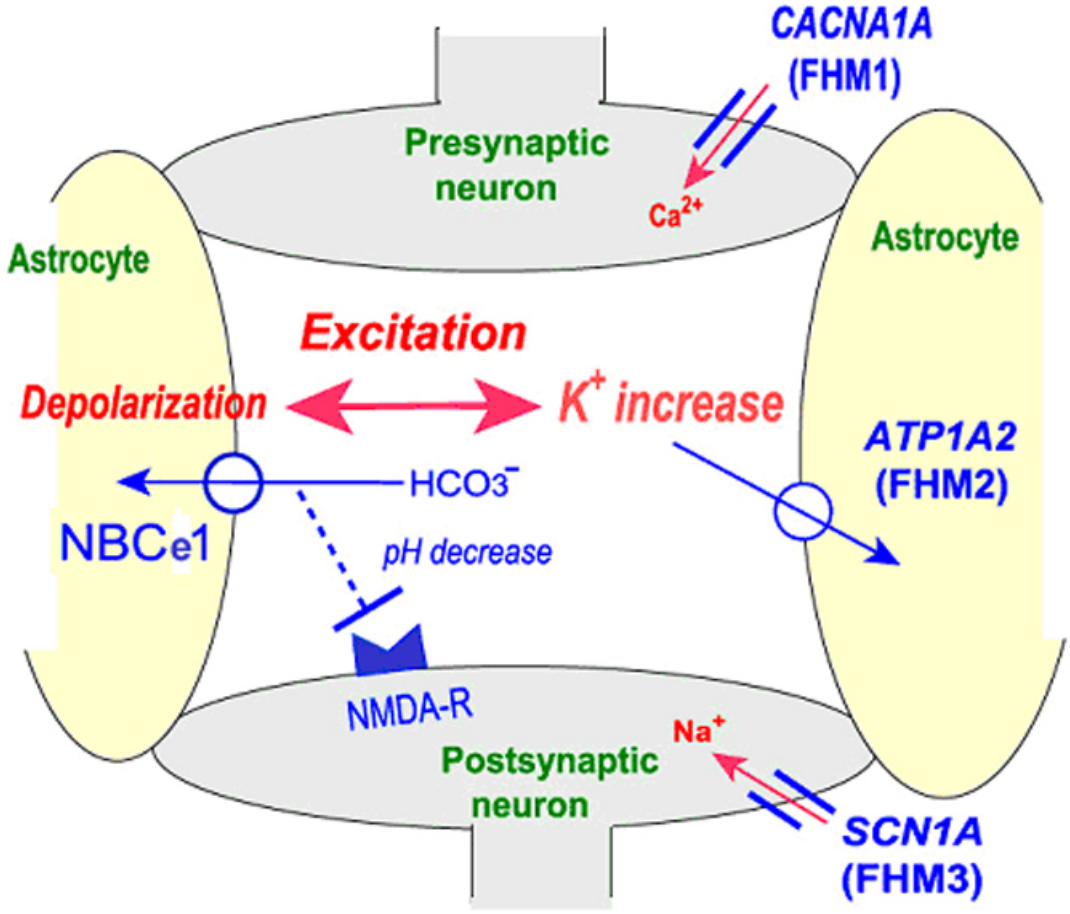
CACNA1A
(FHM1)
Presynaptic
neuron
Ca2+
Astrocyte
Astrocyte
Excitation
Depolarization
K+ increase
ATP1A2
(FHM2)
HCO3−
NBCe1
pH decrease
NMDA-R
Na+
Postsynaptic
neuron
SCN1A
(FHM3)

Fig. 2

a

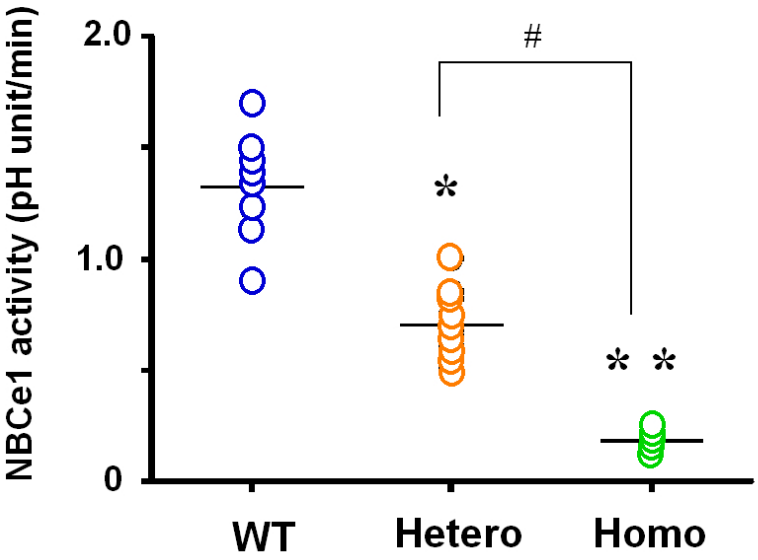
NBCe1 activity (pH unit/min)
2.0
1.0
0
#
*
* *
WT
Hetero
Homo

b

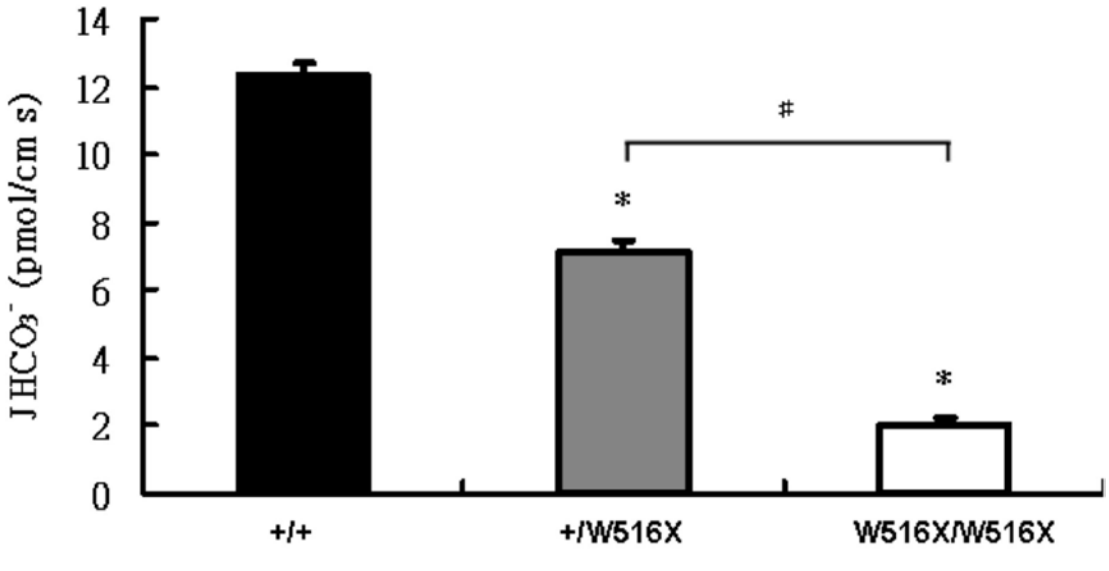
JHCO3- (pmol/cm s)
14
12
10
8
6
4
2
0
#
*
*
+/+
+/W516X
W516X/W516X

Fig. 3

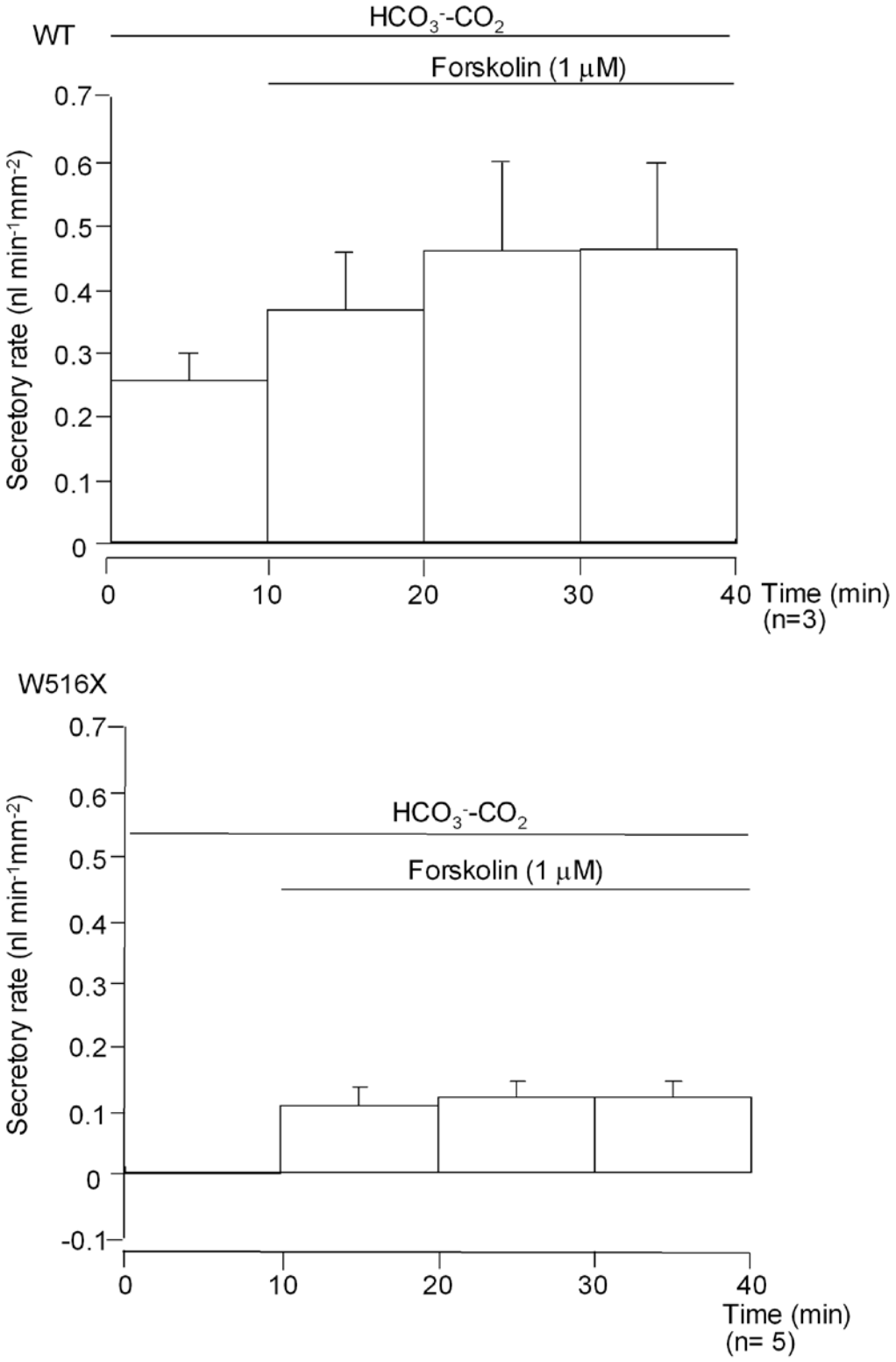
WT
HCO3--CO2
Forskolin (1 μM)
Secretory rate (nl min-1mm-2)
0.7
0.6
0.5
0.4
0.3
0.2
0.1
0
0
10
20
30
40
Time (min)
(n=3)
W516X
HCO3--CO2
Forskolin (1 μM)
Secretory rate (nl min-1mm-2)
0.7
0.6
0.5
0.4
0.3
0.2
0.1
0
-0.1
0
10
20
30
40
Time (min)
(n= 5)

Fig. 4

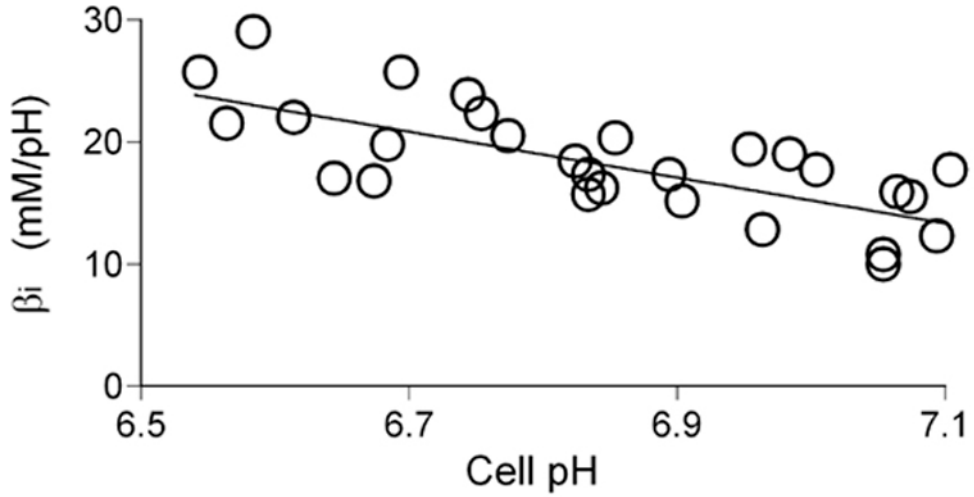

Fig. 5

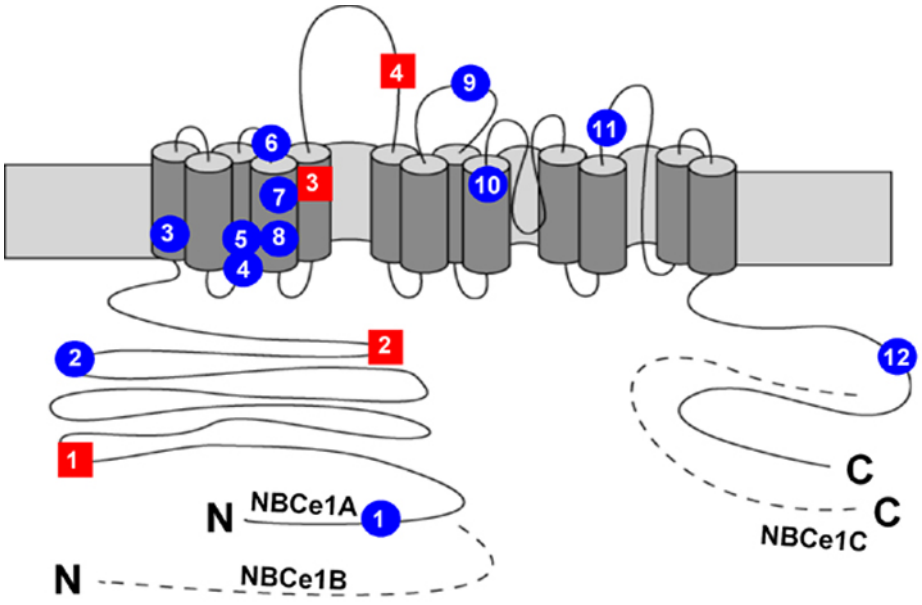

Fig. 6

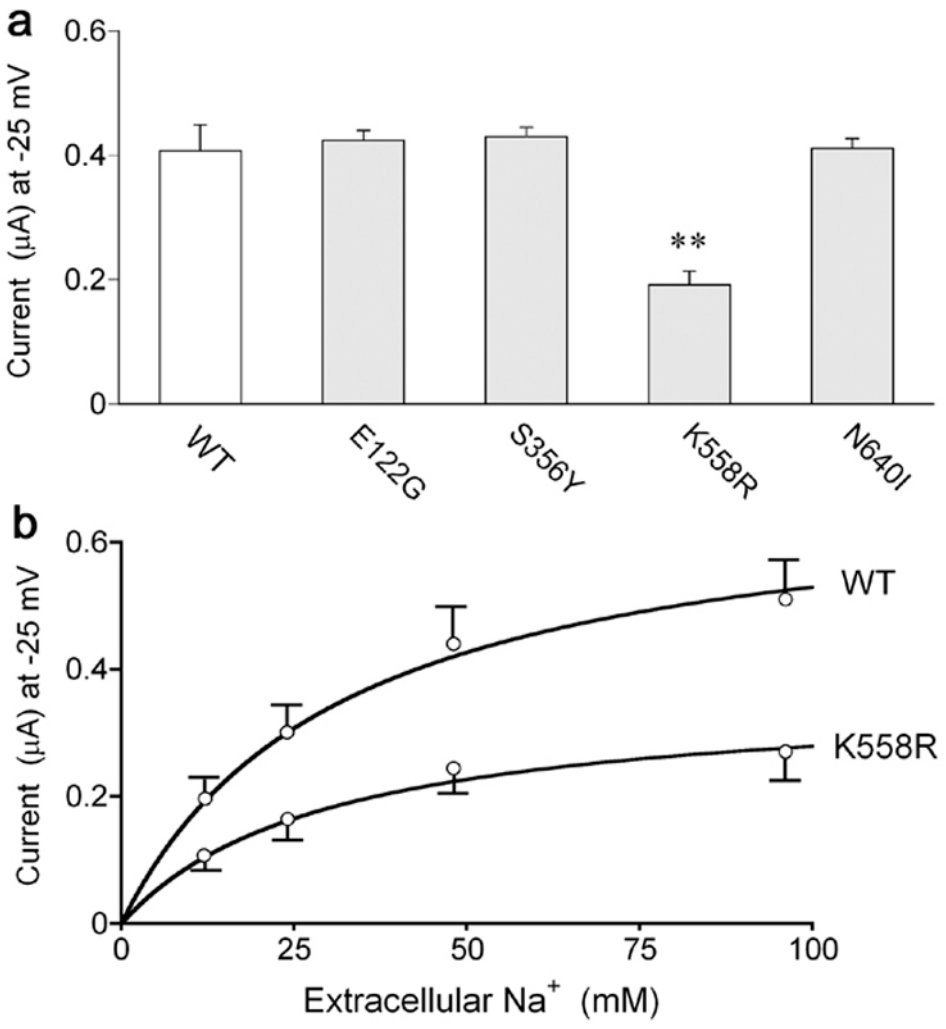
a
Current (μA) at -25 mV
0.6
0.4
0.2
0
**
WT
E122G
S356Y
K558R
N640I
b
Current (μA) at -25 mV
0.6
0.4
0.2
0
WT
K558R
0
25
50
75
100
Extracellular Na+ (mM)

Fig. 7

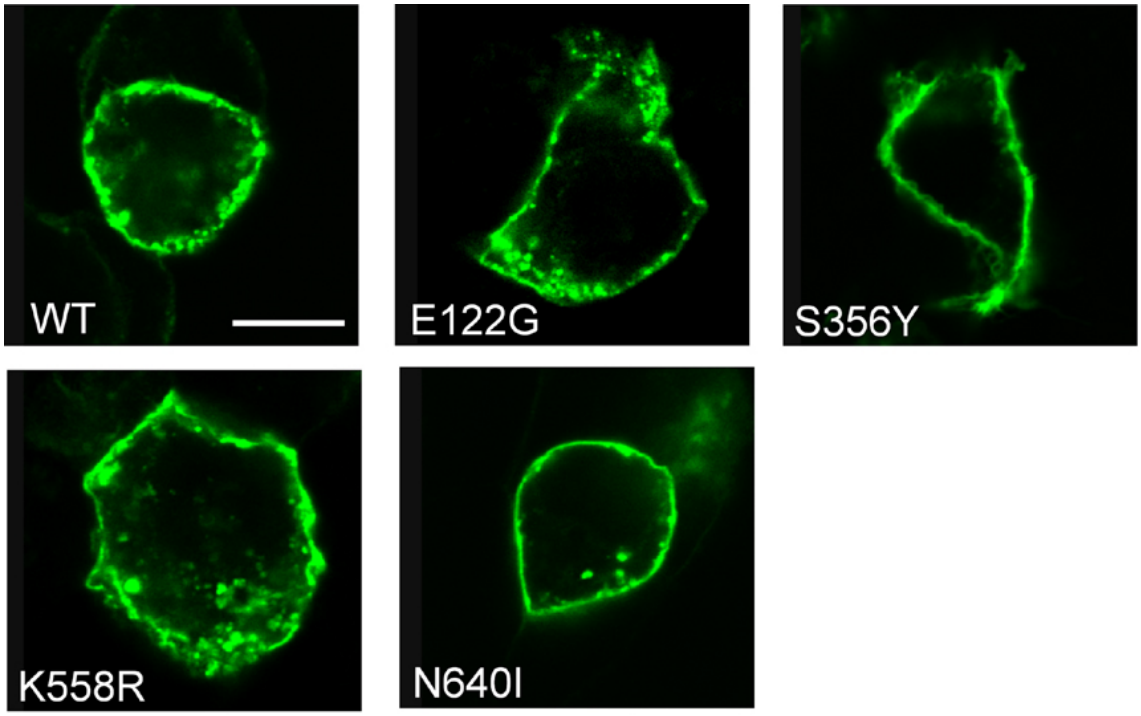

Fig. 8

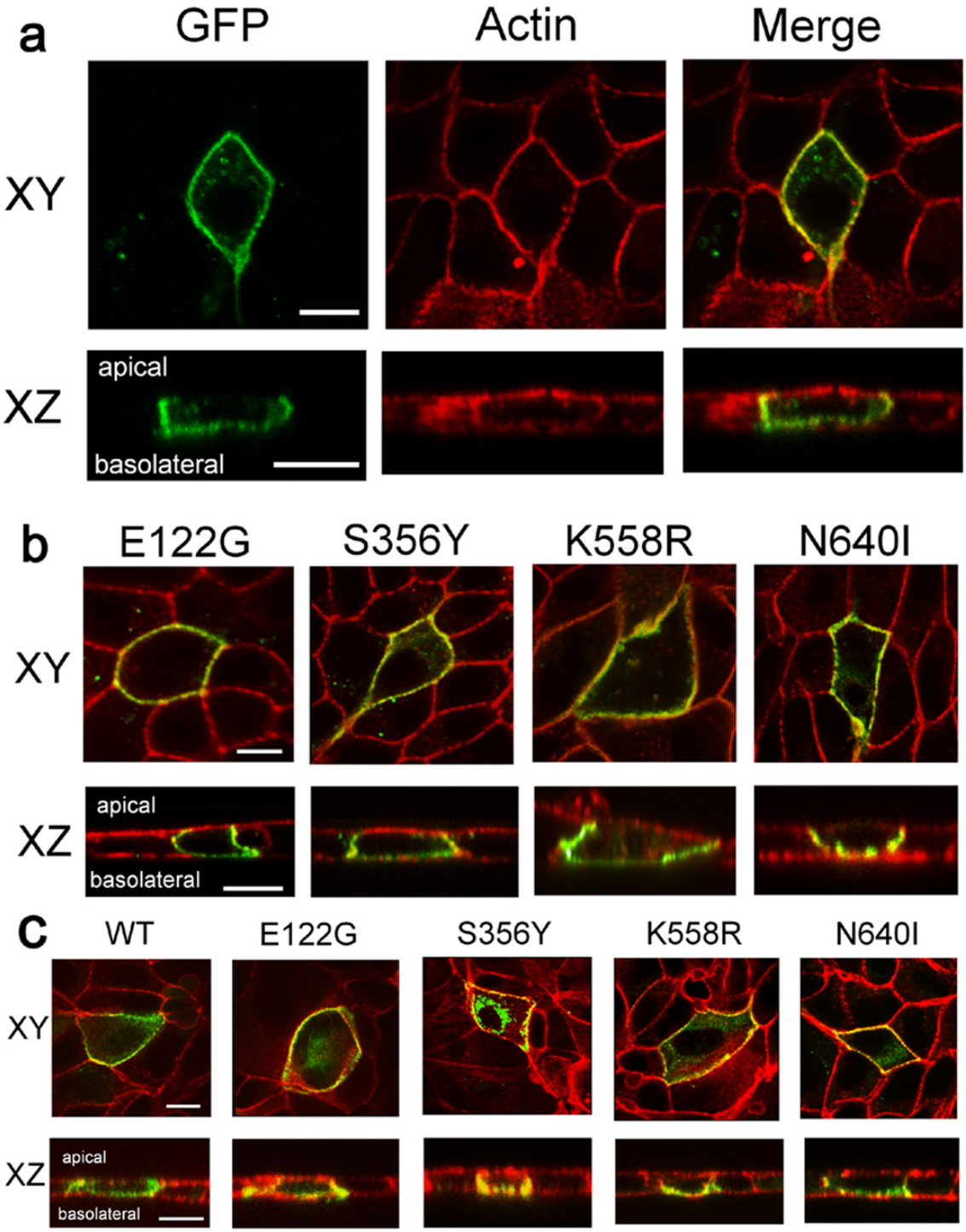
a
GFP
Actin
Merge
XY
XZ
apical
basolateral
b
E122G
S356Y
K558R
N640I
XY
XZ
apical
basolateral
C
WT
E122G
S356Y
K558R
N640I
XY
XZ
apical
basolateral

Fig. 9

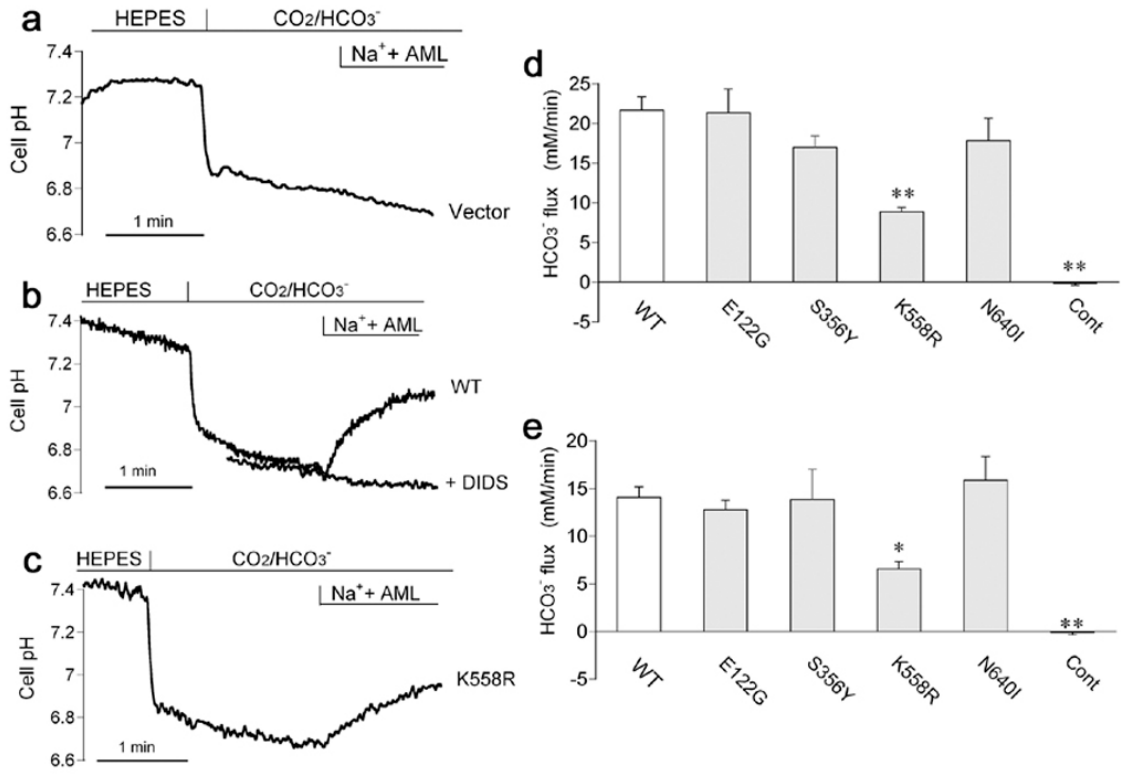
a
HEPES
CO2/HCO3-
Na+ + AML
Cell pH
7.4
7.2
7
6.8
6.6
1 min
Vector
b
HEPES
CO2/HCO3-
Na+ + AML
Cell pH
1 min
WT
+ DIDS
c
HEPES
CO2/HCO3-
Na+ + AML
Cell pH
1 min
K558R
d
HCO3- flux (mM/min)
25
20
15
10
5
0
-5
**
**
WT
E122G
S356Y
K558R
N640I
Cont
e
HCO3- flux (mM/min)
20
15
10
5
0
-5
*
**
WT
E122G
S356Y
K558R
N640I
Cont

Fig. 10

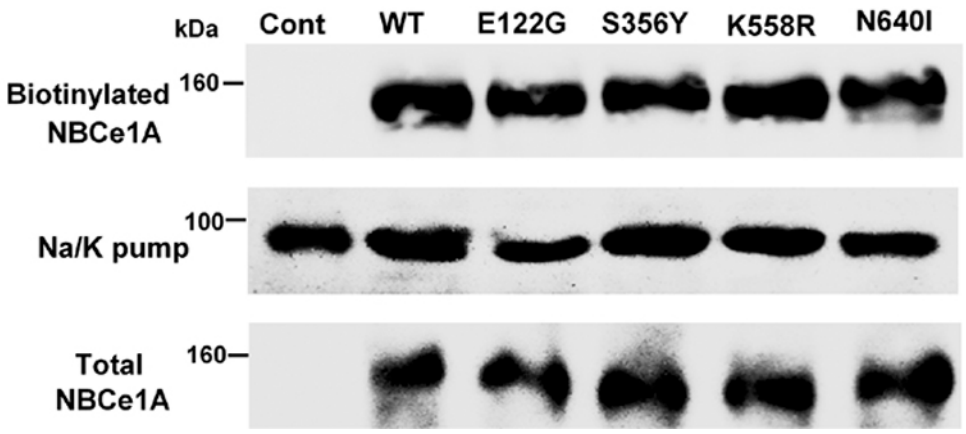
kDa
Cont
WT
E122G
S356Y
K558R
N640I
Biotinylated NBCe1A
160
Na/K pump
100
Total NBCe1A
160

Fig. 11

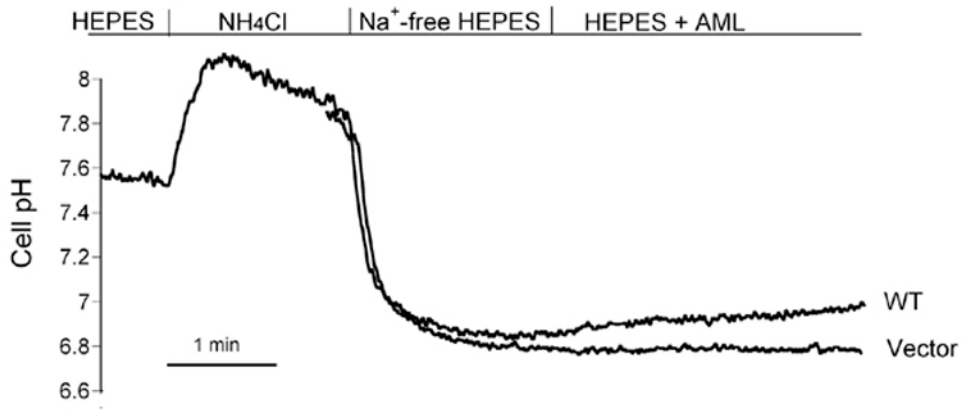
HEPES
NH4Cl
Na+-free HEPES
HEPES + AML
Cell pH
8
7.8
7.6
7.4
7.2
7
6.8
6.6
1 min
WT
Vector

Fig. 12